ACS NANO
Cite This: ACS Nano 2019, 13, 8784–8792
www.acsnano.org

ARTICLE

High Aspect Ratio β-Ga_2O_3 Fin Arrays with Low-Interface Charge Density by Inverse Metal-Assisted Chemical Etching

Hsien-Chih Huang,[†,#] Munho Kim,[†,#,▽] Xun Zhan,[‡] Kelson Chabak,[§] Jeong Dong Kim,[†] Alexander Kvit,[∥] Dong Liu,[⊥] Zhenqiang Ma,[∥,⊥] Jian-Min Zuo,[‡] and Xiuling Li*[,†]

[†]Department of Electrical and Computer Engineering, Micro and Nanotechnology Laboratory, University of Illinois at Urbana—Champaign, Urbana, Illinois 61801, United States

[‡]Department of Materials Science and Engineering, Materials Research Laboratory, University of Illinois, Urbana, Illinois 61801, United States

[§]Air Force Research Laboratory, Sensors Directorate, Wright-Patterson AFB, Wright-Patterson AFB, Ohio 45433, United States

[∥]Department of Materials Science and Engineering, University of Wisconsin—Madison, Madison, Wisconsin 53706, United States

[⊥]Department of Electrical and Computer Engineering, University of Wisconsin—Madison, Madison, Wisconsin 53706, United States

Supporting Information

ABSTRACT: **β-Ga_2O_3, with a bandgap of ~4.6–4.9 eV and readily available bulk substrates, has attracted tremendous interest in the wide bandgap semiconductor community. Producing high aspect ratio β-Ga_2O_3 3D nanostructures without surface damage is crucial for next-generation power electronics. However, most wet etching methods can only achieve very limited aspect ratios, while dry etch usually damages the surface due to high energy ions. In this work, we demonstrate the formation of β-Ga_2O_3 fin arrays on a (010) β-Ga_2O_3 substrate by metal-assisted chemical etching (MacEtch) with high aspect ratio and sidewall surfaces with excellent quality. The etching was found to be strongly crystal orientation dependent, and three kinds of vertical structures were formed after MacEtch. The Schottky barrier height (SBH) between Pt and various MacEtch-produced β-Ga_2O_3 surfaces and sidewalls was found to decrease as the aspect ratio of the β-Ga_2O_3 vertical structure increased. This could be attributed to the different amount of oxygen lost at the surface after etching, as indicated by the XPS and TEM examination. Very little hysteresis was observed in the capacitance–voltage characteristics for the 3D Pt/Al_2O_3/β-Ga_2O_3 MOS capacitor structures, and the extracted interface trap density was as small as 2.73×10^{11} cm^{-2} eV^{-1}, comparable to or lower than that for unetched planar β-Ga_2O_3 surfaces.**

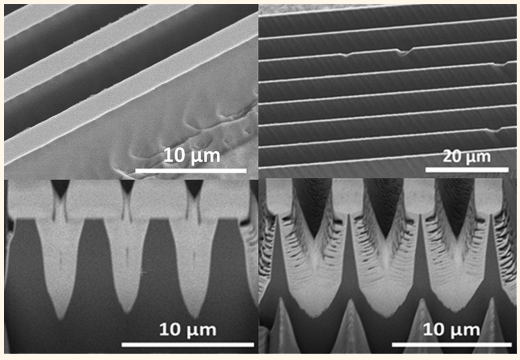

KEYWORDS: *β-Ga_2O_3, metal-assisted chemical etching, high aspect ratio, XPS, Schottky barrier height, D_{it}*

β-Gallium oxide (β-Ga_2O_3) is considered a promising material for high-power applications due to its ultrawide band gap of 4.6–4.9 eV,[1,2] high theoretical breakdown electric field of 8 MV/cm, and reasonable 150 cm^2/V-s electron mobility.[3] These properties lead to a 1721 Baliga's figure of merit for the powering switch and outperforms the value of SiC and GaN.[4−6] Moreover, β-Ga_2O_3 is a wide bandgap semiconducting material with the availability of single crystalline bulk substrate and controllable *n*-type doping concentration over the full range of $<10^{14}$ and up to $>10^{20}$ cm^{-3}.[7,8] Over the past five years, many high-power β-Ga_2O_3 applications, such as Schottky diodes,[9,10] MESFETs,[11] MOSFETs,[12−15] vertical transistors,[16−18] and FinFETs,[19] have been successfully demonstrated. However, the β-Ga_2O_3 transistors published so far still suffer from low current density compared to GaN devices. To further enhance the on-current and gate control, the development of techniques for fabricating β-Ga_2O_3 vertical structures with high aspect ratios (ARs) and smooth surfaces is essential. 3D β-Ga_2O_3 nanostructures will also be useful for solar-blind photodetectors and sensing applications.[20,21]

Although inductively coupled plasma reactive ion etching (ICP-RIE) of β-Ga_2O_3 has been recently studied with surface

Received: March 3, 2019
Accepted: June 17, 2019
Published: June 17, 2019

DOI: 10.1021/acsnano.9b01709
ACS Nano 2019, 13, 8784–8792

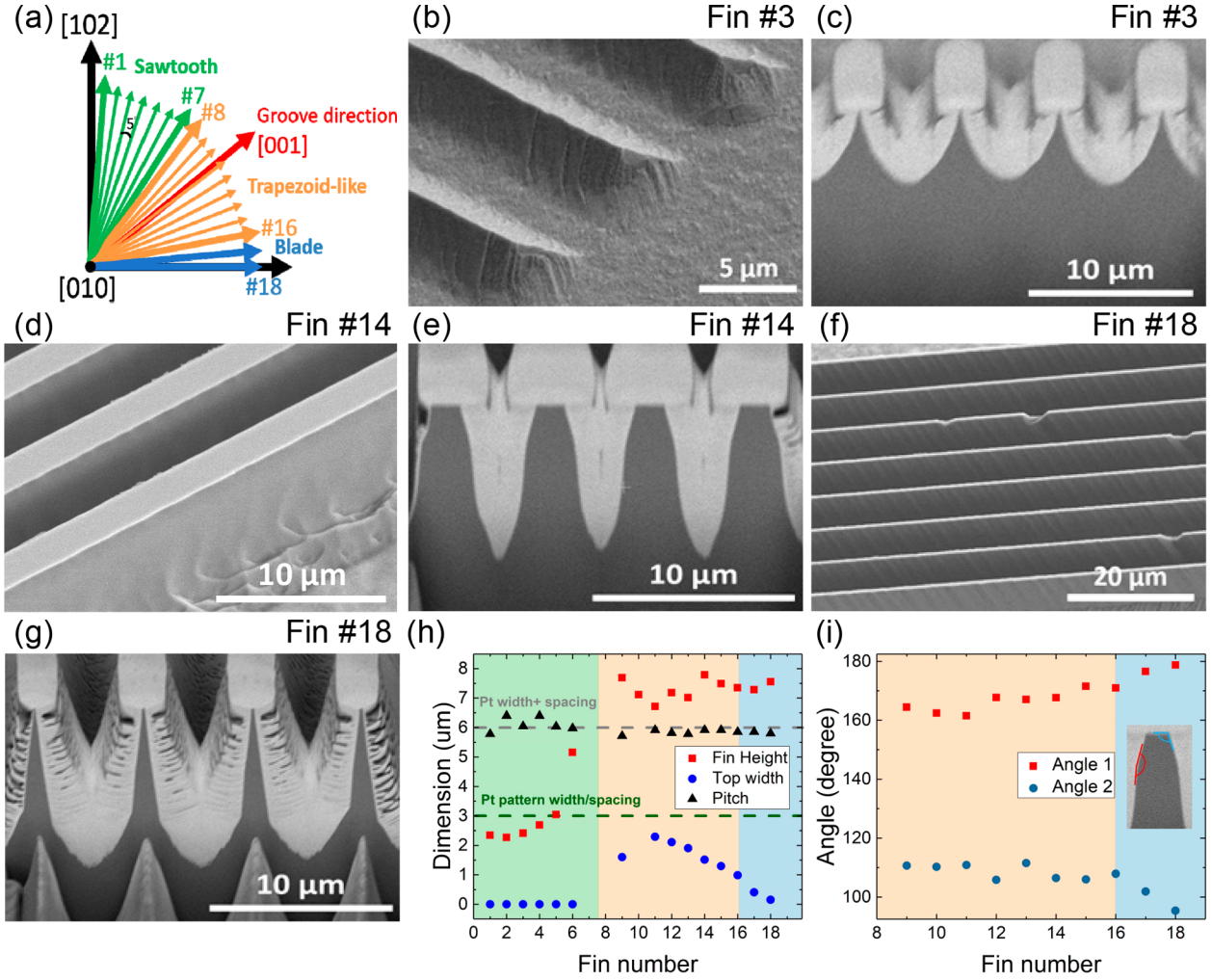

Figure 1. (a) Schematic illiustration of the positions (fin #1 - 18) of the patterned rectagular Pt catalyst strips (representated by arrowed lines originating from the origin), which rotate every 5° from #1 to #18, relative to crystal orientation [102] on a (010) β-Ga_2O_3 substrate. Pt catalyst fin #1 - 7 (green colored), #8 - 16 (orange colored), and #17 - 18 (blue colored) produced three distinct vertical β-Ga_2O_3 structures with sawtooth, trapezoid-like, and blade shaped cross-sectional profiles, respectively. . The red arrow indicates the orientation of the β-Ga_2O_3 nanogrooves . (b–g): 45°-tilted (b, d, f) and cross-sectional (c, e, g) SEM micrographs of β-Ga_2O_3 vertical fin array structures produced by 120 h MacEtch, with (b, c) pyramid (b, c), trapezoid-like (d, e), and blade (f, g) shaped cross-sectional profiles, The Pt catalyst strips were removed before SEM. In the cross-section images (c, e, g), the dark regions are the β-Ga_2O_3 vertical structures and the bright regions covering the structures are Pt protection layers deposited during the FIB process. (h) Plots of β-Ga_2O_3 fin height (red square symbol), top width (blue dot symbol), pitch (black triangle symbol), and (i) angles between upper and lower sidewalls (angle 1) and between the top plane and upper sidewall (angle 2) of β-Ga_2O_3 vertical structures as a function of the Pt catalyst position (Fin number shown in(a)). Green and gray dashed lines in (h) indicate the width or spacing (3 μm each) and the sum of spacing and width (i.e., pitch, 6 μm) of the patterned Pt catalyst strips used in the MacEtch process, respectively.

roughness and etch rate characterization,[22] the etching quality is still limited compared to the GaN etching technologies[23,24] and the highest AR reported so far is only around 2.42.[16] In addition, the surface suffers from high energy ion induced damage, especially at increased etch rate.[19,25] On the other hand, although using the wet etching process might be able to avoid the high-energy ion induced damage caused by dry etching, a high etching temperature (~150 °C) was typically required,[26−28] and the AR achieved was mostly below 1,[27] which is much lower than that of wet etching of GaN.[29−31] Thus, etching techniques that can produce high AR and damage-free surface are urgently needed for this wide bandgap material.

In this work, we demonstrate β-Ga_2O_3 fin arrays produced by metal-assisted chemical etching (MacEtch) with high AR and low interface trap density. The etching behavior as a function of the catalytic metal mask placement with respect to the β-Ga_2O_3 crystal orientation is also systematically investigated. In addition, Schottky barrier height (SBH), surface chemical composition, crystal structure, and surface quality of different MacEtch-formed β-Ga_2O_3 vertical structures are characterized and analyzed.

RESULTS AND DISCUSSION

MacEtch with Pt Mesh Pattern. Unintentionally doped (UID) (010) β-Ga_2O_3 substrates were first etched with a mesh platinum (Pt) catalyst pattern (Figure S1a). The region covered by Pt catalyst mesh (smooth region, as labeled) was not etched except for some undercut at the edges, while the areas not covered by Pt (Pt mesh holes) showed a clear loss of material, demonstrating the inverse MacEtch (i-MacEtch) nature[32,33] under this etching condition (Figure S1b,c). A

DOI: 10.1021/acsnano.9b01709
ACS Nano 2019, 13, 8784−8792

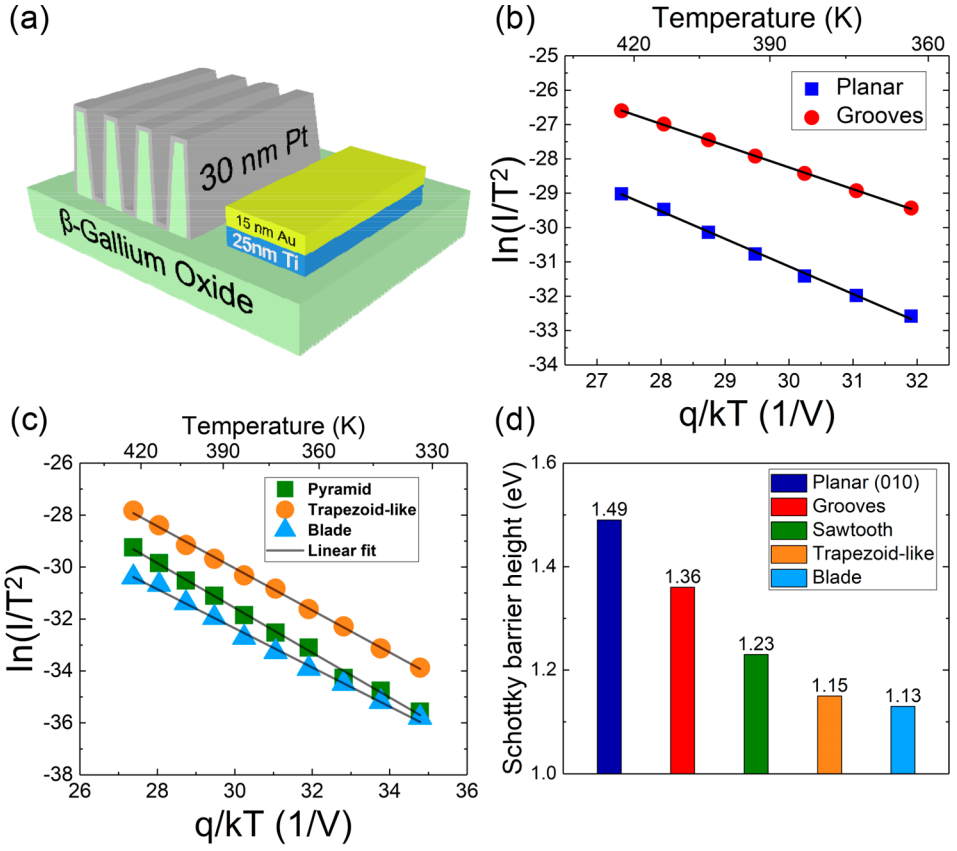

Figure 2. (a) Schematic diagram of Pt/β-Ga_2O_3 Schottky diodes with MacEtch-formed β-Ga_2O_3 vertical structures. (b) $\ln(I/T^2)$ *vs* q/kT plot of Pt/β-Ga_2O_3 Schottky diodes with planar (unetched) and nanogrooves structures. (c) $\ln(I/T^2)$ *vs* q/kT plot of Pt/β-Ga_2O_3 Schottky diodes with pyramid, trapezoid-like, and blade shaped structures. The ideality factor of the Schottky diodes with planar, grooves, pyramid, trapezoid-like, and blade structures was extracted to be 1.17, 1.09, 1.18, 1.1 and 1.06, respectively. (d) The extracted Schottky barrier height with planar, grooves, pyramid, trapezoid-like, and blade structures.

control experiment without the presence of the Pt pattern was conducted , and no etching was observed under the same etching condition (Figure S1d), confirming the metal-assisted mechanism in this etching process. In contrast to i-MacEtch of InP and Ge, where smooth sidewalls were formed,[33,34] curvilinear nanoscale grooves were observed for β-Ga_2O_3 i-MacEtch.[35] These nanogrooves, ~100 nm tall and spaced by 180 nm, were distributed in all open (not covered by Pt) regions and mostly aligned in the [001] orientation.[35] The nanogrooved structure has been characterized by atomic force microscopy and used as surface texture to enhance the photoresponsivity of β-Ga_2O_3 photodiode.[35] Aligned nanogrooves have also been reported in RIE dry etching of β-Ga_2O_3.[22] Furthermore, pits with similar shape and orientation have been observed in as-grown (010) β-Ga_2O_3 single crystals.[34]

MacEtch with Pt Fin Pattern: Orientation Dependence. To study the crystal orientation dependence of i-MacEtch of this material system, systematic etching experiments were carried out on β-Ga_2O_3 using arrays of rectangular fin-shaped patterns of Pt catalyst arranged in a fanlike pattern in 5° increment rotation angle away from the [102] direction (#1−18, as illustrated in Figure 1a). A strong dependence of etching behavior on the Pt catalyst pattern orientation is found. The 3D vertical structures produced can be classified into three major categories based on their cross-sectional geometrical profiles: pyramid, trapezoid-like, and blade structures, which correspond to Pt catalyst strip orientations of #1−7, #8−16, and #17−18, respectively, as labeled in Figure 1a.

Parts b−g of Figure 1 show the tilted view and FIB cross-sectional view SEM images of the three distinct sets of resultant structures. For etching using Pt catalyst fin orientation of 5 to 35° away from [102], *i.e.*, fins #1−7 in Figure 1a, an array of pyramid-like vertical β-Ga_2O_3 structures, with the top clearly pinched off, was formed after MacEtch (Figure 1b,c). The sidewalls of the pyramid structure appear to be curved with no uniquely identifiable single crystal planes but clear roughness featuring aligned nanogrooves, similar to those previously reported.[35] In contrast, for etching using Pt catalyst fin orientation of 40−80° from [102] (*i.e.*, fins #8−16 in Figure 1a), as shown in Figure 1d, e, a trapezoid-like shaped β-Ga_2O_3 etching profile with well-defined top surface and sidewall facets was produced. Note that the 20 nm thick Pt catalyst strips remain on top of these vertical structures after MacEtch as a result of i-MacEtch. Moreover, unlike the pyramid structure which was covered with nanogrooves on the surface, a smoother and steeper sidewall was achieved in the trapezoid-like structure. Finally, with the orientation of 85 to 90° away from [102] (fins #17−18 in Figure 1a), an ultrahigh AR and blade shaped structure was produced after Macetch, as shown in Figure 1f,g. It can be seen that there is only one plane on the sidewalls of this blade structure, instead of two etching planes observed in the trapezoid-like structure. From the tilted SEM image, some shallow grooves can be observed on the sidewalls. With the metal catalyst pattern in the fin #18 direction, the

DOI: 10.1021/acsnano.9b01709
ACS Nano 2019, 13, 8784−8792

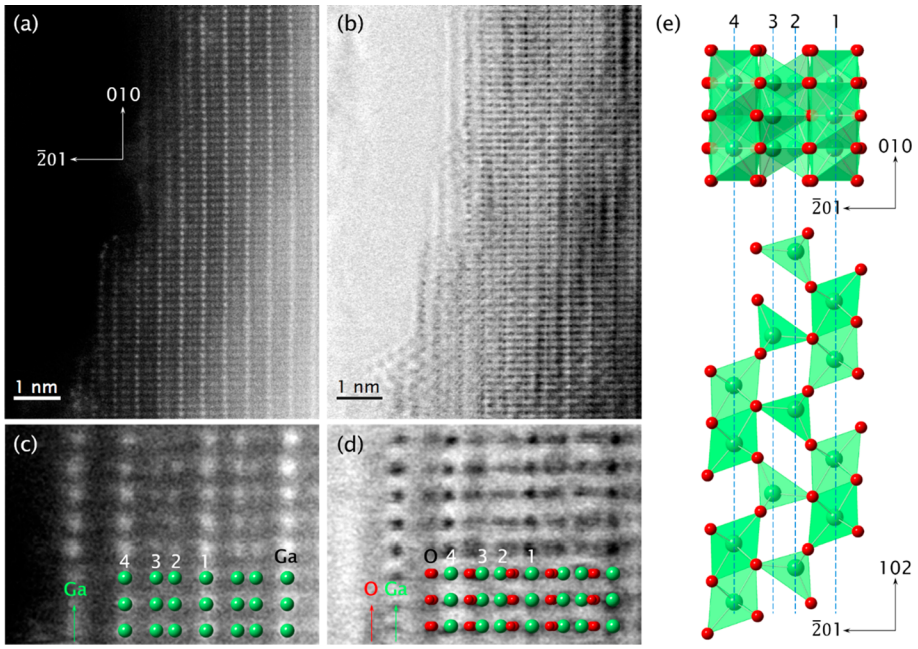

Figure 3. (a) STEM-HAADF image of surface structure of β-Ga_2O_3. The zone axis is [102]. (b) Corresponding STEM-ABF image. (c, d) Enlarged HAADF and ABF images, respectively, overlapping with projected crystal structure model along [102]. (e) Projected structure model along [102] and [010].

average height of the structure is around 7.55 μm but with only a 151 nm top width, which is the highest fin height among all published β-Ga_2O_3 vertical structures. Note that a similar crystallographic dependence of etching profile was observed in the wet etching of β-Ga_2O_3 and the photoelectrochemical etching of TiO_2.[36] To the best of our knowledge, this is the only demonstration of β-Ga_2O_3 fin array with below 200 nm fin top width, over 7 μm fin height, and smooth sidewalls by any etching techniques.

The top width, pitch, and height of the MacEtch-formed β-Ga_2O_3 structures in each fin orientation are plotted in Figure 1h. The pitch of all the structures are around 6 μm, which matches the sum of Pt bar width and the spacing between them (gray dash line in Figure 1h). The height of pyramid structures with orientation close to the [102] direction is about 2.5 μm and increases with transit to the trapezoid-like structure. For trapezoid-like and blade shaped structures, the heights are close to 7 μm with around 1 μm variation, showing a roughly 58 nm/h vertical etching rate under this etching condition. The top is pinched off in the pyramid structures, giving a zero top width. As the angle between fin orientation and [102] direction increases, the top width also increases and reaches a maximum value of 2.29 μm at Fin #11. The top width subsequently decreases as the fin orientation rotates away from [102] and reaches a minimum value of 151 nm at Fin #18 in the blade structure, producing the highest AR among all MacEtch-formed β-Ga_2O_3 vertical structures. Note that the Pt catalyst pattern used to generate this structure is 3 μm wide and limits the spacing between fins. Hence, further explorationof theetching process window to reduce the undercut is still required in order to produce a denser array of β-Ga_2O_3 fins.

Figure 1i shows the top angle and the angle between two etching planes on the sidewalls of trapezoid-like and the blade shaped structures. The average top angle in the fin orientation #9−16 remains at around 110°, generating a trapezoid-like shape in these orientations. However, the top angle decreases in Fins #17−18 as the angle between fin orientation and [102] direction increases and drops to around 90° in Fin #18, producing a more vertical sidewall compared to the trapezoid-like structure. As for the angle between the two etching planes on the sidewall, it slowly increases as the fin orientation rotates away from [102] and reaches a maximum value of 180° in Fin #18, where the two sidewall etching planes merge into one plane.

The strong crystallographic dependence of etching can be attributed to the number of oxygen dangling bonds on different crystal planes. It has been reported that [$\bar{2}$ 01] β-Ga_2O_3 substrates have a higher etching rate than [010] substrates with KOH-based wet etching due to more oxygen dangling bonds on the [$\bar{2}$ 01] plane.[28] With the asymmetric monoclinic crystal structures of β-Ga_2O_3, the number of oxygen dangling bonds on each plane varies,[28,36] resulting in some planes being more chemically stable than others. Consequently, the etching profile produced by MacEtch would be highly dependent on how the Pt catalyst pattern is spatially laid out on the surface relative to the crystal orientation.

Schottky Barrier Characterization of the MacEtched β-Ga_2O_3 surface. To characterize the surface property of vertical β-Ga_2O_3 structures formed by MacEtch, a 30 nm thick Pt film was deposited conformally on these 3D structures usingan e-beam evaporator (Figure S2), forming a Schottky contact at the interface between Pt and β-Ga_2O_3 (Figure 2a), while the Ohmic contact was formed on the side of the fin array using Ti/Au (25 nm/15 nm). Current−voltage characteristics under different temperatures (323−423 K in increment of 10k) was measured for the samples with pyramid, trapezoid-like, and blade-shaped β-Ga_2O_3 structures, as well as the unetched planar (010) substrate and that covered with uniform shallow nanogrooves (Figure S2). All samples demonstrated Schottky-like current−voltage characteristics

DOI: 10.1021/acsnano.9b01709
ACS Nano 2019, 13, 8784−8792

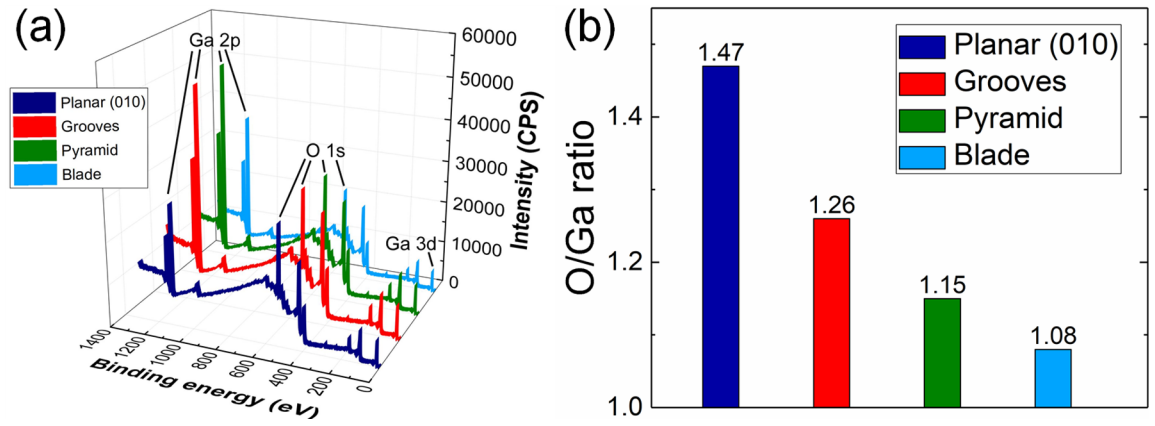

Figure 4. XPS characterization of surface with planar (unetched) and MacEtch-formed structures. (a) XPS survey scan. (b) O/Ga ratio of different β-Ga_2O_3 structures extracted through the O 1s and Ga 3d peak intensity.

and ideality factors between 1.06 to 1.18 (Figure S3). Using the thermionic emission model,[37] the current−voltage behavior for Schottky contact above room temperature can be described as

$$I = AA^*T^2 e^{-q\Phi_B/nkT}(e^{qV/nkT} - 1) \quad (1)$$

where q is the electron charge, A is the area of Schottky contact, A^* is the Richardson constant, and Φ_B is the SBH, n is the ideality factor, k is the Boltzmann constant, and T is the temperature. Dividing the current I by T^2, eq 1 can be written as

$$\ln\left(\frac{I}{T^2}\right) = \ln(AA^*) - q(\Phi_B - V/n)/kT \quad (2)$$

Therefore, the SBH can be extracted from the slope of the $\ln(I/T^2)$ *vs* q/kT plot. Parts b and c of Figure 2 show the comparison of $\ln(I/T^2)$ *vs* q/kT at 0.4 V for the samples with planar, nanogrooved surfaces, and all three 3D structures formed by MacEtch. All the curves in Figure 2b,c demonstrate excellent linearity with coefficient of determination (R^2) over 0.995, giving a highly accurate extraction of SBHs. The extracted SBHs between Pt and β-Ga_2O_3 with different structures are shown in Figure 2d. Note that the extracted value of the SBH between Pt and (010) planar surface matches well with other published values in the literature.[38] For all the interfaces between Pt and the MacEtched surface formed, the SBHs were less than 1.49 eV of planar (010) surface by at least 0.13 eV. As the AR of the β-Ga_2O_3 structures increases, the SBH decreases, reaching as low as 1.13 eV with the blade shaped structure.

TEM and XPS Characterization of the MacEtched β-Ga_2O_3 Surface. To understand the origin of the reduction of SBHs after etching, the MacEtch-formed β-Ga_2O_3 surface was examined by the STEM. Note the samples were transferred to TEM *via* air; thus the surface might be passivated. Parts a and b of Figure 3 show the HAADF and ABF images, respectively, of MacEtch β-Ga_2O_3 shown in Figure 1f,g, along the [102] direction. It can be seen that the sidewall of the etched structure is composed of steps of $\{\bar{2}\,01\}$ planes. Parts c and d of Figure 3 are the HAADF and ABF images recorded at high magnification from a region near the surface, providing detailed atomistic structure information. In Figure 3c, "bright" contrast corresponds to Ga atom columns. In Figure 3d, "dark" contrast corresponds to Ga and O atoms columns. By combining parts c and d of Figure 3, both Ga and O are clearly resolved. The structure of β-Ga_2O_3 belongs to the space group of $C2/m$. Its crystal structure contains the GaO_6 octahedron and the GaO_4 tetrahedron. The structure as projected along [102] is shown at the top of Figure 3e. The Ga atomic positions in a unit cell are marked by lines 1−4 from right to left and named Ga1−Ga4. The projected atomic structure models without and with oxygen atoms are superimposed on the atomic resolution images of parts c and d, respectively, of Figure 3. The comparison clearly shows that the surface is not terminated with the bulk unit cell structure. On the contrary, it terminates with a Ga−O layer, while the Ga atoms are clearly resolved, the surface O layer is diffuse and not individually resolved, as seen in Figure 3d. The projection distance between the surface Ga layer and sublayer Ga4 coincides with the distance from Ga1 to Ga3, that is, the surface Ga sites coincides with the Ga3 sites. Ga3 is tetrahedrally coordinated as seen in Figure 3e. Although the Ga3 seems to be separate from Ga1 in HAADF and ABF images, it actually connects with Ga1, as shown in Figure 3e, along [010] zone axis, which is a 90° rotation along $[\bar{2}01]$. The projection distance between surface O and surface Ga3 is different from those of inside (Figure S4), suggesting a different structure, which we could call as reconstruction. The presence of the surface O layer indicates a passivated surface, with neighboring GaO_4 tetrahedra sharing O atoms, leading to an O deficiency and reducing the dangling bonds at the surface. This finding further supports the previous hypothesis of the crystal orientation dependent etching since the higher etching rate might be attributed to more dangling bonds on the surface plane.[28,39] The reduction of dangling bonds due to surface reconstruction would result in a more chemically stable plane, which matches with the previous etching results.

In addition to the TEM characterization, the surface chemical composition of unetched (010) planar β-Ga_2O_3 and vertical structures produced by MacEtch was inspected with XPS. Figure 4a shows the XPS survey scan of β-Ga_2O_3 with planar, nanogrooves, pyramid, trapezoid-like, and blade structure. No peak position change was found after MacEtch or among different etch formed structures, while a clearintensity reductionof O 1s peak was observed after MacEtch in all three structures. The composition ratio between O and Ga atoms was calculated with O 1s and Ga 3d peak signal and plotted in Figure 4b. Note that the O/Ga ratio of unetched planar β-Ga_2O_3 is around 1.47, which is close to the stoichiometric value of 1.5. The composition O/Ga ratio of

DOI: 10.1021/acsnano.9b01709
ACS Nano 2019, 13, 8784−8792

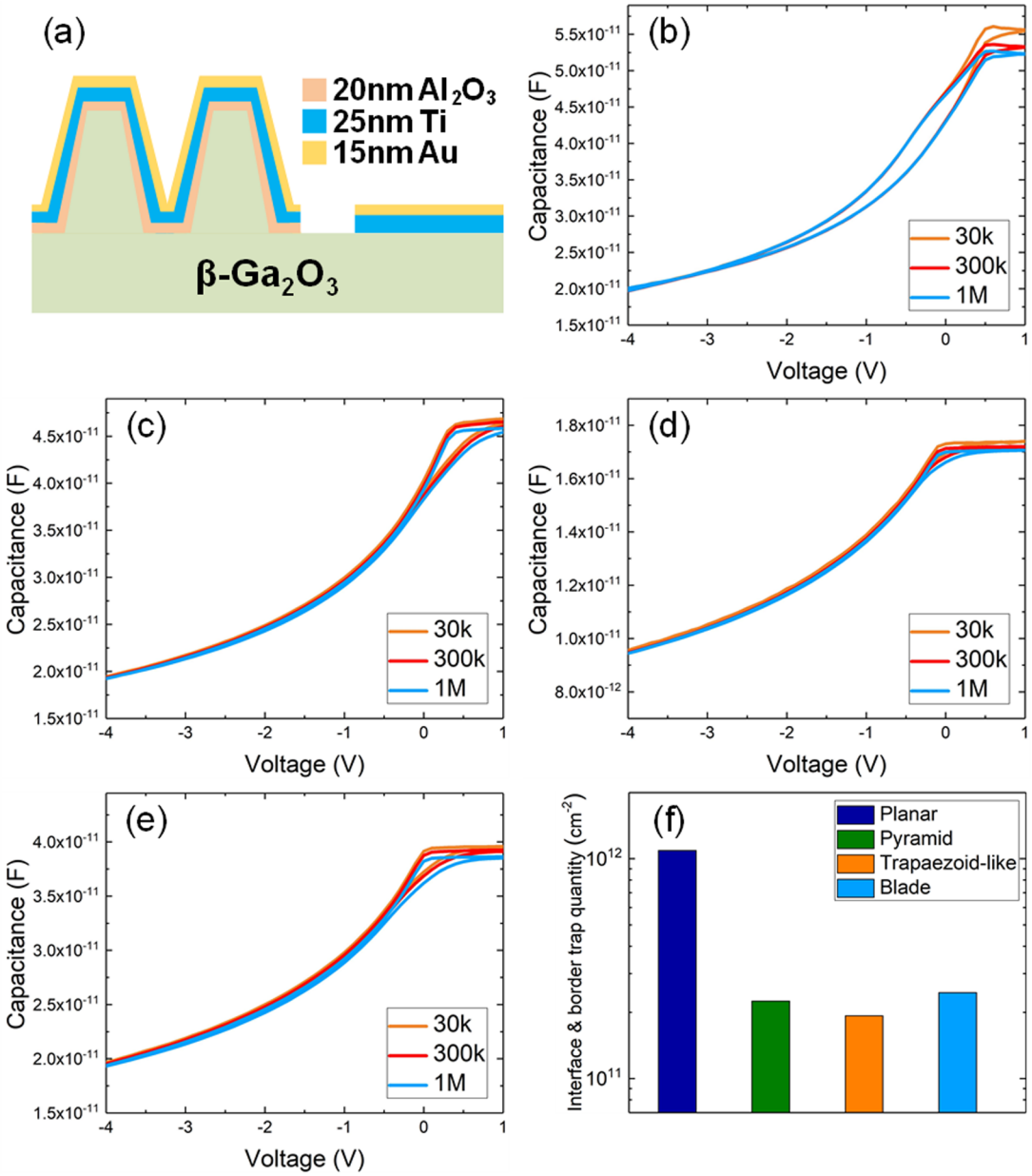

Figure 5. (a) Schematic diagram of Au/Ti/Al_2O_3/β-Ga_2O_3 MOSCAP with MacEtch-formed β-Ga_2O_3 vertical structures. The Ti/Au electrode on the side is used for Ohmic contact with the substrate. Frequency-dependent $C-V$ measurements of Au/Ti/Al_2O_3/β-Ga_2O_3 MOSCAPs with (b) unetched planar, (c) pyramid, (d) trapezoid-like, and (e) blade structures formed by 120 h MacEtch. (e) Extracted interface and border trap quantity of β-Ga_2O_3 MOSCAPs with (b-e) structures.

etched β-Ga_2O_3 shows a decrease from 1.5 to 1.26, 1.15, and 1.08 with grooves, pyramid, and blade structures, respectively, demonstrating the same trend as the reduction of SBHs with different structures (Figure 2d) and is consistent with the surface O contraction previously observed in the TEM images. Moreover, the reduced band gap energy of oxygen deficient β-Ga_2O_x layer due to increasing electron affinity has been reported,[40] which could be the reason for the decreased SBH between Pt and etched β-Ga_2O_3 surface (Figure 2d).

CV Characterization of MOSCAP Interfaces. To further investigate the interface quality of the MacEtch produced 3D structures, a 20 nm Al_2O_3 layer and Ti/Au metal electrode were deposited on these etch-formed vertical structures by atomic layer deposition (ALD) and e-beam evaporation, respectively, forming a MOS capacitor (MOSCAP), as illustrated in Figure 5a. The frequency-dependent C−V hysteresis curves of planar and different MacEtch-formed β-Ga_2O_3 structures are shown in Figure 5b−e. The biasing starts from negative voltage (depletion) to positive voltage (accumulation), then sweep back to depletion. Due to the trapping and detrapping of the traps through the dual sweeps, a flat-band voltage (V_{FB}) shift is generated. The flat-band capacitance hysteresis of planar, pyramid, trapezoid-like, and blade structures are 0.434, 0.09, 0.077, and 0.098 V, respectively, and has been previously attributed to the interface traps and border traps in accumulation.[19,41,42] Through the V_{FB} shift in the $C-V$ curve, the detectable interface and border trap quantity (Q_t) can be estimated by the following equation

$$Q_t = C_{ox} \times \Delta V / q \quad (3)$$

DOI: 10.1021/acsnano.9b01709
ACS Nano 2019, 13, 8784−8792

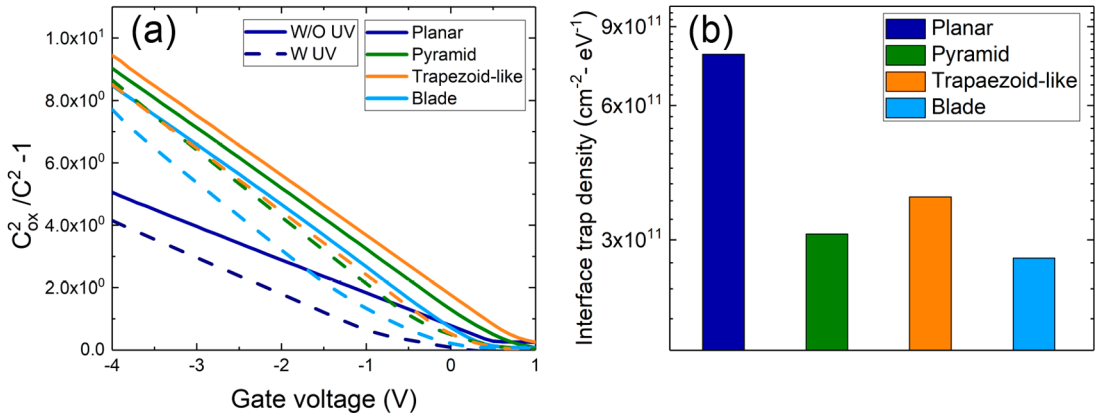

Figure 6. (a) $C_{ox}^2/C^2 - 1$ *vs* gate voltage plot and (b) extracted interface trap density of Au/Ti/Al_2O_3/β-Ga_2O_3 MOSCAPs with planar, pyramid, trapezoid-like, and blade structures formed by 120 h MacEtch. The measured capacitance before and after 10 min UV illumination are labeled as solid and dashed lines in (a), respectively; and the upward shift of the curves after UV illumination is because the interface traps become donor-dominated instead of the previous acceptor-dominated condition. Note that the flat band voltage value is extracted through extrapolating $C_{ox}^2/C^2 - 1$ *vs* gate voltage at $C_{ox}^2/C^2 - 1 = 0$; and the slope of the planar structure is slightly lower than other structures, due to the carrier concentration difference between UID β-Ga_2O_3 samples.

where C_{ox} is the oxide capacitance and ΔV is the flat-band voltage difference. As shown in Figure 5f, all Q_t decreased after the MacEtch process and reached a lowest value of 1.93×10^{11} cm^{-2} with the trapezoid-like structure. Note that here the theoretical C_{ox} value (0.4 $\mu F/cm^2$) was used by using 9.1 as the dielectric constant and 20 nm as the nominal thickness of Al_2O_3 for calculation. The actual C_{ox} are typically lower than the theoretical value, thus, this would lead to an overestimated Q_t when applying eq 3. Even with this overestimation, the MacEtch-formed structures still demonstrate comparable Q_t values ($(1.9-2.5) \times 10^{11}$ cm^{-2}) to other published unetched result (3.2×10^{11} cm^{-2}),[43] showing that the etched β-Ga_2O_3 surfaces with good quality are formed after the MacEtch process. Moreover, no obvious frequency dispersion or stretch out can be observed in the $C-V$ curves of all the MacEtch-formed β-Ga_2O_3 structures, further confirming the good interface quality. However, Q_t only shows the amount of trap states close to the band edge and with the wide bandgap property of this material, the MOS interface trap density (D_{it}) over the entire bandgap would be more accurate to reflect the surface quality of the MacEtched structures. Due to the large band gap of β-Ga_2O_3, photoassisted $C-V$ method is considered as a more reliable approach to extract the average D_{it} compared to Hi/Lo or Terman methods.[43] This method is based on obtaining the V_{FB} shift in $C-V$ curves of interface traps filled with electrons and holes to extract the D_{it}.[41,43] The average D_{it} can be expressed as the following equation

$$D_{it} = \frac{C_{OX} \cdot \Delta V}{q \cdot E_g} \tag{4}$$

where C_{ox} is the oxide capacitance, ΔV is the V_{FB} shift, and E_g is the bandgap of β-Ga_2O_3. The V_{FB} is determined through extrapolating $C_{ox}^2/C^2 - 1$ *vs* gate voltage at $C_{ox}^2/C^2 - 1 = 0$ (Figure 6a). Figure 6b shows the extracted D_{it} with planar and all the MacEtch-formed structures and demonstrates a similar result as the Q_t with different structures (Figure 5f). All of the structures after MacEtch exhibit a lower D_{it} than the unetched planar sample. This reduction in D_{it} can be attributed to the contraction of dangling bonds due to surface reconstruction after MacEtch process. The achieved minimum D_{it} is 2.73×10^{11} cm^{-2} eV^{-1} with the blade structure. Note that the theoretical C_{ox} (0.4 $\mu F/cm^2$) is still used in eq 4, which leads to an overestimation of the extracted D_{it}. Still, the MacEtch-formed interfaces exhibit comparable D_{it} values ($(2.73-3.74) \times 10^{11}$ cm^{-2} eV^{-1}) to other published result (2.3×10^{11} cm^{-2} eV^{-1}),[43] confirming that the MacEtch process is capable of fabricating β-Ga_2O_3 nanostructures with both ultrahigh AR and low interface-trap surface for device applications.

CONCLUSION

In conclusion, we have demonstrated β-Ga_2O_3 fin arrays produced by MacEtch with high aspect ratio and excellent surface quality. The etching isfound to be strongly crystal orientation dependent under the slow etch condition used here. Three kinds of 3D vertical structures, with pyramid, trapezoid-like, and blade shaped cross-sectional profiles, are produced. The SBHs between Pt and the 3D β-Ga_2O_3 surfaces decrease as the AR of the β-Ga_2O_3 vertical structure increases, consistent with the loss of oxygen (XPS) and the surface reconstruction (TEM). The CV measurements on all the 3D Al_2O_3/β-Ga_2O_3 MOSCAP structures only show a small amount of hysteresis and the minimum extracted interface trap density is only 2.73×10^{11} cm^{-2} eV^{-1}, which is comparable to or even better than other published results using planar β-Ga_2O_3 surface and our own unetched control samples. This proves the capability of MacEtch process for fabricating β-Ga_2O_3 nanostructures with both ultrahigh AR and excellent interface quality suitable for device applications. Although there is much more to be developed in MacEtch of β-Ga_2O_3, including enhancing the etch rate, we believe this work represents a significant step in achieving β-Ga_2O_3 3D transistors and photodetectors as well as other 3D structure-based devices beyond the current wide bandgap semiconductor materials for power electronics and optoelectronics applications.

EXPERIMENTAL METHODS

Unintentionally doped (UID) (010) β-Ga_2O_3 substrates with doping levels of $(0.8-8.0) \times 10^{17}$ cm^{-3} were used for all etching experiments. The substrate was diced into 5×5 mm^2 squares. Prior to metal patterning, all β-Ga_2O_3 samples were thoroughly cleaned with acetone, IPA, and DI water. Then, the samples were patterned by nanosphere lithography with 500 nm diameter spheres or standard

DOI: 10.1021/acsnano.9b01709
ACS Nano 2019, 13, 8784−8792

photolithography, followed by e-beam evaporation of a 20 nm thick Pt film. The formed Pt pattern was either mesh with 500 nm diameter circular spacing (as illustrated in Figure S2) or an array of 500 μm long bars with 3 μm width and 3 μm spacing.

The β-Ga_2O_3 samples with the Pt pattern were immersed in a mixture of hydrofluoric acid (HF, 49%) and potassium persulfate ($K_2S_2O_8$) with a molar concentration of 0.28 M and 0.18 mM, respectively, under the illumination of a 254 nm ultra violet (UV) lamp at room temperature. The distance between the UV source and β-Ga_2O_3 sample was ~6 cm and the etching solution was refreshed every 24 h. The etching profile was characterized with scanning electron microscopy (SEM, Hitachi S-4700) in both top and tilted view. Cross-sectional view of the etched structures was inspected with dual-beam focus ion beam (FIB)/SEM system (Thermo Scios2). Surface stoichiometry and chemical composition of planar and etched β-Ga_2O_3 were examined with X-ray photoelectron spectroscopy (XPS, Kratos Axis ULTRA). Scanning transmission electron microscope (STEM) images were acquired using a Themis Z analytical (S)TEM (Thermo Fisher) operating at 300 kV and with a probe aberration corrector and the HAADF detector, as well as the segmented detectors (DF4 and DF2). At the imaging camera length, the HAADF collection angle range was 50−200 mrad, while the range for ABF was 10−20 mrad. By combining HAADF and ABF, the Ga and O atomic columns were resolved and identified at the same time. For the β-Ga_2O_3 MOSCAP fabrication, a piranha pretreatment was conducted prior to the 20 nm Al_2O_3 deposition with ALD (Cambridge NanoTech) at 250 °C. Then, a post deposition annealing at 480 °C with N_2 ambient for 1 min was performed, followed by a 25 nm Ti and 15 nm Au electrode deposition with e-beam evaporator.

For the hysteresis and frequency dispersion CV measurement, the DC sweep rate was 1 s per 0.1 V step, and the hysteresis and Q_t wereextracted fromthe 1 MHz results. For the UV-assisted CV measurement, the MOS capacitors were first bias at accumulation (V_G = 2 V) for 10 s to fill the traps with electrons, and then the gate bias wasswept from accumulation to deep depletion with 1 MHz AC frequency. Then, the MOSCAP wasilluminated with a 254 nm UV lampand biased at deep depletion (−6 V) for 7 min to fill the traps with holes. Finally, the UV illumination wasturned off and the gate bias wasswept from deep depletion to accumulation. The D_{it} wasextracted using the saturated capacitance value under accumulation bias condition as the oxide capacitance (C_{ox}) for each of the MacEtch-formed structure and this value wasused in the normalization of $C_{ox}^2/C^2 - 1$. The flat band voltages werecalculated by extrapolation of the linear region (around −4 to −1 V in Figure. 6a) at $C_{ox}^2/C^2 - 1 = 0$. Since the C_{ox} here wasextracted from the same MacEtch-formed structure and has the identical device area, D_{it} can still be extracted without knowing the actual device area.

ASSOCIATED CONTENT

Supporting Information

The Supporting Information is available free of charge on the ACS Publications website at DOI: 10.1021/acsnano.9b01709.

SEM images of β-Ga_2O_3 surface after MacEtch with Pt mesh catalyst pattern, SEM images of Pt/β-Ga_2O_3 Schottky diodes, current−voltage characteristics of β-Ga_2O_3 Schottky diodes under different temperatures, STEM-HAADF image and line profiles of Ga/O atoms at MacEtched β-Ga_2O_3 surface, SEM images of β-Ga_2O_3 sample without and with Pt catalyst on top after 4 h MacEtch, SEM images of whole β-Ga_2O_3 sample with arrays of fins in different orientations, schematic diagram of the hypothesized β-Ga_2O_3 MacEtch process, and UV-assisted capacitance−voltage measurements of β-Ga_2O_3 MOSCAPs with different MacEtch-formed structures (PDF)

AUTHOR INFORMATION

Corresponding Author

*E-mail: xiuling@illinois.edu.

ORCID

Hsien-Chih Huang: 0000-0002-3783-5517
Munho Kim: 0000-0002-0379-1886
Zhenqiang Ma: 0000-0001-9214-1342
Jian-Min Zuo: 0000-0002-5151-3370
Xiuling Li: 0000-0003-3698-5182

Present Address

[▽](M.K.) School of Electrical and Electronic Engineering, Nanyang Technological University, 50 Nanyang Avenue, 639798 Singapore, Singapore.

Author Contributions

[#]H.-C.H. and M.K. contributed equally.

Notes

The authors declare no competing financial interest.

ACKNOWLEDGMENTS

This material is based upon work supported in part by the National Science Foundation under Grant No. 18-09946. X.Z. was supported by the Center for Emergent Superconductivity, an Energy Frontier Research Center funded by the US Department of Energy, Office of Science, Office of Basic Energy Sciences, under Award No. DE-AC0298CH10886.

REFERENCES

(1) Higashiwaki, M.; Jessen, G. H. Guest Editorial: The Dawn of Gallium Oxide Microelectronics. *Appl. Phys. Lett.* **2018**, *112*, 060401.

(2) He, H.; Orlando, R.; Blanco, M. A.; Pandey, R.; Amzallag, E.; Baraille, I.; Rérat, M. First-Principles Study of the Structural, Electronic, and Optical Properties of Ga_2O_3 in Its Monoclinic and Hexagonal Phases. *Phys. Rev. B: Condens. Matter Mater. Phys.* **2006**, *74*, 195123.

(3) Ma, N.; Tanen, N.; Verma, A.; Guo, Z.; Luo, T.; Xing, H.; Jena, D. Intrinsic Electron Mobility Limits in β-Ga_2O_3. *Appl. Phys. Lett.* **2016**, *109*, 212101.

(4) Rafique, S.; Han, L.; Tadjer, M. J.; Freitas, J. A.; Mahadik, N. A.; Zhao, H. Homoepitaxial Growth of β-Ga_2O_3 Thin Films by Low Pressure Chemical Vapor Deposition. *Appl. Phys. Lett.* **2016**, *108*, 182105.

(5) Tadjer, M. J.; Anderson, T. J.; Feygelson, T. I.; Hobart, K. D.; Hite, J. K.; Koehler, A. D.; Wheeler, V. D.; Pate, B. B.; Eddy, C. R.; Kub, F. J. Nanocrystalline Diamond Capped AlGaN/GaN High Electron Mobility Transistors *via* a Sacrificial Gate Process. *Phys. Status Solidi A* **2016**, *213*, 893−897.

(6) Kodama, M.; Sugimoto, M.; Hayashi, E.; Soejima, N.; Ishiguro, O.; Kanechika, M.; Itoh, K.; Ueda, H.; Uesugi, T.; Kachi, T. GaN-Based Trench Gate Metal Oxide Semiconductor Field-Effect Transistor Fabricated with Novel Wet Etching. *Appl. Phys. Express* **2008**, *1*, No. 021104.

(7) Leedy, K. D.; Chabak, K. D.; Vasilyev, V.; Look, D. C.; Boeckl, J. J.; Brown, J. L.; Tetlak, S. E.; Green, A. J.; Moser, N. A.; Crespo, A.; Thomson, D. B.; Fitch, R. C.; Mccandless, J. P.; Jessen, G. H. Highly Conductive Homoepitaxial Si-Doped Ga_2O_3 Films on (010) β-Ga_2O_3 by Pulsed Laser Deposition. *Appl. Phys. Lett.* **2017**, *111*, 12103.

(8) Murakami, H.; et al. Homoepitaxial Growth of β-Ga2O3 Layers by Halide Vapor Phase Epitaxy. *Appl. Phys. Express* **2015**, *8*, 15503.

(9) Li, W.; Hu, Z.; Nomoto, K.; Zhang, Z.; Hsu, J.-Y.; Thieu, Q. T.; Sasaki, K.; Kuramata, A.; Jena, D.; Xing, H. G. 1230 V β-Ga_2O_3 Trench Schottky Barrier Diodes with an Ultra-Low Leakage Current of <1 μ A/cm^2. *Appl. Phys. Lett.* **2018**, *113*, 202101.

DOI: 10.1021/acsnano.9b01709
ACS Nano 2019, 13, 8784−8792

(10) Yang, J.; Ren, F.; Tadjer, M.; Pearton, S. J.; Kuramata, A. 2300V Reverse Breakdown Voltage Ga_2O_3 Schottky Rectifiers. *ECS J. Solid State Sci. Technol.* **2018**, *7*, Q92−Q96.
(11) Xia, Z.; Joishi, C.; Krishnamoorthy, S.; Bajaj, S.; Zhang, Y.; Brenner, M.; Lodha, S.; Rajan, S. Delta Doped β-Ga_2O_3 Field Effect Transistors With Regrown Ohmic Contacts. *IEEE Electron Device Lett.* **2018**, *39*, 568−571.
(12) Si, M.; Yang, L.; Zhou, H.; Ye, P. D. β-Ga_2O_3 Nanomembrane Negative Capacitance Field-Effect Transistors with Steep Subthreshold Slope for Wide Band Gap Logic Applications. *ACS Omega* **2017**, *2*, 497136.
(13) Chabak, K. D.; McCandless, J. P.; Moser, N. A.; Green, A. J.; Mahalingam, K.; Crespo, A.; Hendricks, N.; Howe, B. M.; Tetlak, S. E.; Leedy, K.; Fitch, R. C.; Wakimoto, D.; Sasaki, K.; Kuramata, A.; Jessen, G. H. Recessed-Gate Enhancement-Mode β-Ga_2O_3 MOSFETs. *IEEE Electron Device Lett.* **2018**, *39*, 67−70.
(14) Noh, J.; Si, M.; Zhou, H.; Tadjer, M. J.; Ye, P. D. The Impact of Substrates on the Performance of Top-Gate β-Ga_2O_3 Field-Effect Transistors: Record High Drain Current of 980 mA/mm on Diamond. In *2018 76th Device Research Conference (DRC)*; IEEE, 2018; pp 1−2.
(15) Joishi, C.; Xia, Z.; Mcglone, J.; Zhang, Y.; Arehart, A. R.; Ringel, S.; Lodha, S.; Rajan, S. Effect of Buffer Iron Doping on Delta-Doped β-Ga_2O_3 Metal Semiconductor Field Effect Transistors. *Appl. Phys. Lett.* **2018**, *113*, 123501.
(16) Hu, Z.; Nomoto, K.; Li, W.; Tanen, N.; Sasaki, K.; Kuramata, A.; Nakamura, T.; Jena, D.; Xing, H. G. Enhancement-Mode Ga_2O_3 Vertical Transistors with Breakdown Voltage 1 kV. *IEEE Electron Device Lett.* **2018**, *39*, 869−872.
(17) Hu, Z.; Nomoto, K.; Li, W.; Zhang, Z.; Tanen, N.; Thieu, Q. T.; Sasaki, K.; Kuramata, A.; Nakamura, T.; Jena, D.; Xing, H. G. Breakdown Mechanism in 1 KA/cm ^{2} and 960 V E-Mode β-Ga_2O_3 Vertical Transistors. *Appl. Phys. Lett.* **2018**, *113*, 122103.
(18) Wong, M. H.; Goto, K.; Murakami, H.; Kumagai, Y.; Higashiwaki, M. Current Aperture Vertical β-Ga_2O_3 MOSFETs Fabricated by N- and Si-Ion Implantation Doping. *IEEE Electron Device Lett.* **2019**, *40*, 431−434.
(19) Chabak, K. D.; Moser, N.; Green, A. J.; Walker, D. E.; Tetlak, S. E.; Heller, E.; Crespo, A.; Fitch, R.; McCandless, J. P.; Leedy, K.; Baldini, M.; Wagner, G.; Galazka, Z.; Li, X.; Jessen, G. Enhancement-Mode Ga_2O_3 Wrap-Gate Fin Field-Effect Transistors on Native (100) β -Ga $_2$ O $_3$ Substrate with High Breakdown Voltage. *Appl. Phys. Lett.* **2016**, *109*, 213501.
(20) Zhang, D.; Zheng, W.; Lin, R. C.; Li, T. T.; Zhang, Z. J.; Huang, F. High Quality β-Ga_2O_3 Film Grown with N_2O for High Sensitivity Solar-Blind-Ultraviolet Photodetector with Fast Response Speed. *J. Alloys Compd.* **2018**, *735*, 150−154.
(21) Lin, R.; Zheng, W.; Zhang, D.; Zhang, Z.; Liao, Q.; Yang, L.; Huang, F. High-Performance Graphene/β-Ga_2O $_3$ Heterojunction Deep-Ultraviolet Photodetector with Hot-Electron Excited Carrier Multiplication. *ACS Appl. Mater. Interfaces* **2018**, *10*, 22419−22426.
(22) Yang, J.; Ahn, S.; Ren, F.; Pearton, S.; Khanna, R.; Bevlin, K.; Geerpuram, D.; Kuramata, A. Inductively Coupled Plasma Reactive-Ion Etching of β-Ga_2O_3: Comprehensive Investigation of Plasma Chemistry and Temperature. *J. Vac. Sci. Technol. A Vacuum, Surfaces, Film.* **2017**, *35*, 13504.
(23) Sun, M.; Zhang, Y.; Gao, X.; Palacios, T. High-Performance GaN Vertical Fin Power Transistors on Bulk GaN Substrates. *IEEE Electron Device Lett.* **2017**, *38*, 509−512.
(24) Zhang, Y.; Sun, M.; Liu, Z.; Piedra, D.; Hu, J.; Gao, X.; Palacios, T. Trench Formation and Corner Rounding in Vertical GaN Power Devices. *Appl. Phys. Lett.* **2017**, *110*, 193506.
(25) Yang, J.; Ahn, S.; Ren, F.; Khanna, R.; Bevlin, K.; Geerpuram, D.; Pearton, S. J.; Kuramata, A. Inductively Coupled Plasma Etch Damage in (−201) Ga_2O_3 Schottky Diodes. *Appl. Phys. Lett.* **2017**, *110*, 142101.
(26) Oshima, T.; Okuno, T.; Arai, N.; Kobayashi, Y.; Fujita, S. Wet Etching of β-Ga_2O_3 Substrates. *Jpn. J. Appl. Phys.* **2009**, *48*, 040208.
(27) Higashiwaki, M.; Jessen, G. H ? *Appl. Phys. Lett.* **2018**, *112*, 060401−3118.
(28) Jang, S.; Jung, S.; Beers, K.; Yang, J.; Ren, F.; Kuramata, A.; Pearton, S. J.; Baik, K. H. A Comparative Study of Wet Etching and Contacts on ($2\bar{0}1$) and (010) Oriented β-Ga_2O_3. *J. Alloys Compd.* **2018**, *731*, 118−125.
(29) Granz, T.; Mariana, S.; Hamdana, G.; Yu, F.; Fatahilah, M. F.; Clavero, I. M.; Puranto, P.; Li, Z.; Brand, U.; Prades, J. D.; Peiner, E.; Waag, A.; Wasisto, H. S. Nanofabrication of Vertically Aligned 3D GaN Nanowire Arrays with Sub-50 nm Feature Sizes Using Nanosphere Lift-off Lithography. *Multidiscip. Digit. Publ. Inst. Proc.* **2017**, *1*, 309.
(30) Wan, H.; Tang, B.; Li, N.; Zhou, S.; Gui, C.; Liu, S. Revealing the Role of Sidewall Orientation in Wet Chemical Etching of GaN-Based Ultraviolet Light-Emitting Diodes. *Nanomaterials* **2019**, *9*, 365.
(31) Debnath, R.; Ha, J.-Y.; Wen, B.; Paramanik, D.; Motayed, A.; King, M. R.; Davydov, A. V. Top-down Fabrication of Large-Area GaN Micro-and Nanopillars. *J. Vac. Sci. Technol., B: Nanotechnol. Microelectron.: Mater., Process., Meas., Phenom.* **2014**, *32*, 21204.
(32) Kim, S. H.; Mohseni, P. K.; Song, Y.; Ishihara, T.; Li, X. Inverse Metal-Assisted Chemical Etching Produces Smooth High Aspect Ratio InP Nanostructures. *Nano Lett.* **2015**, *15*, 641−648.
(33) Kim, M.; Yi, S.; Kim, J. D.; Yin, X.; Li, J.; Bong, J.; Liu, D.; Liu, S.-C.; Kvit, A.; Zhou, W.; Wang, X.; Yu, Z.; Ma, Z.; Li, X. Enhanced Performance of Ge Photodiodes *via* Monolithic Antireflection Texturing and α-Ge Self-Passivation by Inverse Metal-Assisted Chemical Etching. *ACS Nano* **2018**, *12*, 6748−6755.
(34) Kong, L.; Song, Y.; Kim, J. D.; Yu, L.; Wasserman, D.; Chim, W. K.; Chiam, S. Y.; Li, X. Damage-Free Smooth-Sidewall InGaAs Nanopillar Array by Metal-Assisted Chemical Etching. *ACS Nano* **2017**, *11*, 10193−10205.
(35) Kim, M.; Huang, H.-C.; Kim, J. D.; Chabak, K. D.; Raj, A.; Kalapala, K.; Zhou, W.; Li, X. Nanoscale Groove Textured β-Ga_2O_3 by Room Temperature Inverse Metal-Assisted Chemical Etching and Photodiodes with Enhanced Responsivity. *Appl. Phys. Lett.* **2018**, *113*, 222104.
(36) Pearton, S. J.; Yang, J.; Cary, P. H.; Ren, F.; Kim, J.; Tadjer, M. J.; Mastro, M. A. A Review of Ga_2O_3 Materials, Processing, and Devices. *Appl. Phys. Rev.* **2018**, *5*, 11301.
(37) Sze, S. M.; Ng, K. K.*Physics of Semiconductor Devices*; Wiley-Interscience, 2007.
(38) Yao, Y.; Gangireddy, R.; Kim, J.; Das, K. K.; Davis, R. F.; Porter, L. M. Electrical Behavior of β-Ga_2O_3 Schottky Diodes with Different Schottky Metals. *J. Vac. Sci. Technol., B: Nanotechnol. Microelectron.: Mater., Process., Meas., Phenom.* **2017**, *35*, 3−113.
(39) Fu, H.; Chen, H.; Huang, X.; Baranowski, I.; Montes, J.; Yang, T.-H.; Zhao, Y. Effect of Crystalline Anisotropy on Vertical ($\bar{2}01$) and (010) Beta-Ga_2O_3 Schottky Barrier Diodes on EFG Single-Crystal Substrates. *IEEE Trans. Electron Dev.* **2018**, *65*, 3507. DOI: 10.1109/TED.2018.2841904
(40) Heinemann, M. D.; Berry, J.; Teeter, G.; Unold, T.; Ginley, D. Oxygen Deficiency and Sn Doping of Amorphous Ga_2O_3. *Appl. Phys. Lett.* **2016**, *108*, No. 022107.
(41) Jayawardena, A.; Ramamurthy, R. P.; Ahyi, A. C.; Morisette, D.; Dhar, S. Interface Trapping in ($\bar{2}01$) β-Ga_2O_3 MOS Capacitors with Deposited Dielectrics. *Appl. Phys. Lett.* **2018**, *112*, 192108.
(42) Kamimura, T.; Sasaki, K.; Wong, M. H.; Krishnamurthy, D.; Kuramata, A.; Masui, T.; Yamakoshi, S.; Higashiwaki, M. Band Alignment and Electrical Properties of Al_2O_3/β-Ga_2O_3 Heterojunctions. *Appl. Phys. Lett.* **2014**, *104*, 192104.
(43) Zhou, H.; Alghamdi, S.; Si, M.; Qiu, G.; Ye, P. D. Al_2O_3/β-Ga_2O_3(−201) Interface Improvement Through Piranha Pretreatment and Postdeposition Annealing. *IEEE Electron Device Lett.* **2016**, *37*, 1411−1414.

DOI: 10.1021/acsnano.9b01709
ACS Nano 2019, 13, 8784−8792